MACROSCOPIC BEHAVIOUR AND FRACTURE MODES OF CFRP PANELS TRANSVERSELY LOADED AT THE CENTRE

V. Lopresto and G. Caprino

Department of Materials and Production Engineering - University of Naples "Federico II", P.le Tecchio 80, 80125 Naples

ABSTRACT

Quasi-static and low-velocity impact tests were carried out on carbon fibre-reinforced panels, loading them at the centre by a transverse load. The panel thickness, tup diameter, and support diameter were varied, in order to observe their effect on the overall force-displacement curve, force at first failure, and delamination extent. Besides, microscopic analyses were performed, to ascertain the progression of damage as a function of the loading conditions. Minor differences were found between the quasi-static and impact response. From the force-displacement curves, the higher energy carrying ability of thicker laminates is associated not only with higher contact forces, but also with larger displacements. The same is true when the tup diameter is increased. The first failure load can be predicted by very simple analytical tools. The data collected on delamination extent seem to support both an energy-based criterion and a force-based criterion for its prediction. The experimental results also witness the difficulty of visual inspection of thick structures, where large delaminated areas may be accompanied by very small indentations.

INTRODUCTION

The specific mechanical properties of carbon fibre-reinforced plastic (CFRP) laminates are very attractive in aircraft, where weight saving is a key factor for successful application. Nevertheless, the vulnerability of these materials to impact, often resulting in substantial loss in strength [1-5], deserves serious considerations, entailing the use of heavy safety factors in design.

To resort to more efficient composite structures, different material-based solutions, including ductile matrices [5,6], interleaving [7], hybridisation [8], stitching [9] and specific reinforcement architectures [4], have been devised. At the same time, strong research efforts have been undertaken, aiming to understand and predict the phenomena occurring during impact, providing effective tools in the design stage.

On the design side, the availability of relationships correlating the impact parameters (impactor shape, mass, and velocity, constraint conditions, target geometry, etc.) with the associated damage in the laminate (delamination extent, indentation, etc.) is fundamental, being the necessary step to be accomplished in order to evaluate the material residual properties.

Among the possible failure phenomena occurring in a laminate, delamination has received major attention, because of its deleterious effect on compression strength. There is quite general agreement on the mechanisms of initiation and growth of this mode of failure [3,10]. However, although some semi-empirical or numerical models have been proposed for its prediction [11,12], even the main factor causing delamination is a matter of debate, with some authors referring to energy [13,14], and others to contact force [15,16]. The same holds for the delamination threshold, that is the impact conditions resulting in delamination initiation.

Another important aspect of impact is indentation, the only damage potentially perceivable by a visual examination. Knowing the energy level resulting in a barely visible impact damage (BVID) and the corresponding strength loss would provide a powerful tool to design safe structures without adversely affecting maintenance costs.

In this work, the results of static and low-velocity impact tests carried out on CFRP panels of different thicknesses, using spherical indenters of different diameters, are presented. The effects of the test conditions on the force-displacement curve, first failure, delamination growth, indentation, and failure modes are discussed. The experimental data generated are

also used to verify simple models devoted to the prediction of some parameters relevant in the study of impact.

MATERIALS AND TEST METHODS

The CFRP panels tested in this work were fabricated by hand laying-up T400/HMF934 prepreg layers and curing them in autoclave at 177°C under 0.7 MPa pressure. The stacking sequence was $[(0,90)_n/+45_n/-45_n]_s$, with n=1 to 4. The round brackets in the lamination sequence denote fabric. The fibre areal weight was 145 g/m^2 in the tape and 193 g/m^2 in the fabric. The nominal thickness of the plates after cure was 0.95, 1.90, 2.85 and 3.80 mm for n=1 to 4, respectively. The fibre content was about 55% by volume.

During all the tests, the specimens were simply supported on a steel plate having a circular opening, and statically loaded at the centre with a hemispherical steel tup. Most of the tests were performed using a support diameter D=50 mm, and some setting D=100 mm. Four tup diameters D_t, in the range 6 to 19.8 mm, were adopted.

The quasi-static tests were carried out on an Instron 1251 servo-hydraulic testing machine in displacement control. The displacement rate was v=1 mm/min, and the deflection was evaluated by the stroke position. Preliminary tests were performed up to complete penetration. The load-displacement curves recorded were used to select appropriate load levels, potentially useful in evidencing the progression of damage in the material. Then, additional test were carried-out up to the load levels previously determined. The energy imparted to each specimen was calculated by integration from its load-displacement diagram.

An instrumented drop weight apparatus type CEAST Fractovis Mk 4 was used to perform the low velocity impact tests. To achieve the desired level of energy, both the drop height and mass were suitably varied. The impact speed was measured by a photo-electric sensor. An appropriate appliance was used to catch the tup after the first strike, avoiding rebound. The contact force during impact was continuously recorded, and integrated according to the well known procedures to obtain the force-displacement curve.

After tests, each specimen was inspected to ascertain eventual visible damage, and the indentation resulting from the tup-material contact was measured by a micrometric dial gauge. Then, the samples were subjected to non-destructive evaluation using an ultrasonic C-scan apparatus, in order to gain information on delamination presence and extent. Some of the samples were sectioned, polished, and observed by optical microscopy.

RESULTS AND DISCUSSION

In general, the loading speed was observed to have a quite negligible effect on the panel response. Therefore, in the following discussion no distinction will be made between the quasi-static and low-velocity impact results, although some differences noticed will be highlighted.

- Force-displacement curves

Fig. 1 shows typical force-displacement (F-d) curves recorded during the mechanical tests up to perforation. In particular, Fig. 1a evidences the effect of the tup diameter, and Fig. 1b the influence of the specimen thickness.

Increasing D_t (Fig. 1a) does not sensibly modify the initial rigidity of the specimens. However, the maximum load, as well as the displacement before perforation, considerably increases with D_t, contributing to the energy absorbing capacity of the structure. These trends compare qualitatively well with those found in [17].

As expected, thicker panels exhibit a higher initial rigidity (Fig. 1b). Further, the larger ability to absorb energy of thicker laminates also depends on both a higher maximum force and a higher displacements involved in the contact history.

Of course, the static F-d curves do not suffer oscillations phenomena, present in the dynamic case. The latter render questionable the individuation of the first failure point

(FFP), often associated with the first sudden load drop [9,17], from the F-d curves obtained under low-velocity conditions. The task is even more difficult for thin laminates, because the load drop becomes lower and lower with decreasing the laminate thickness (arrows in Fig. 1b).
In general, the peak load recorded in the static tests was higher than the one characteristic of the dynamic tests. This phenomenon, which was more evident when thick laminates were concerned, did not result in significant effects of speed on the perforation energy.

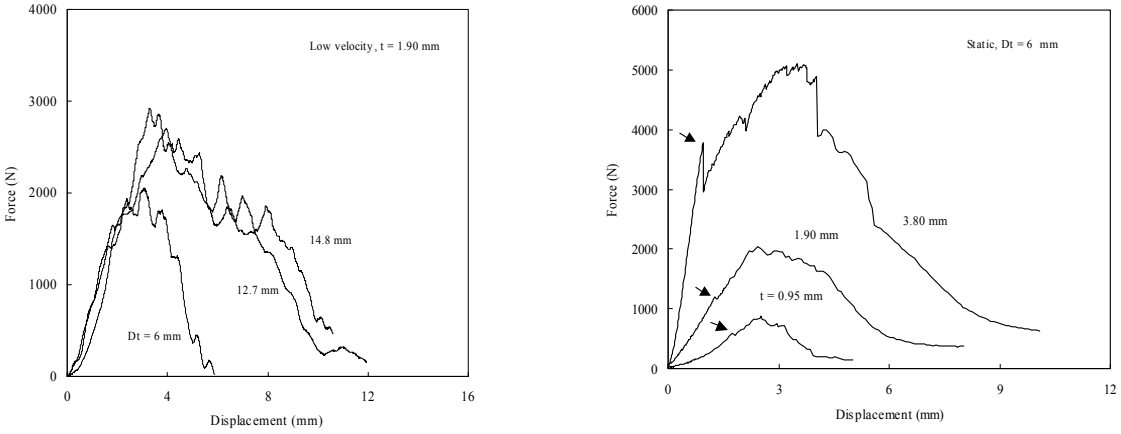

a) b)

Fig. 1 - Effect of: a) the tup diameter, D_t; and, b) specimen thickness, t, on the force-displacement curve.

- First failure force
Different authors have noted that the FFP is a force-dependent, rather than an energy-dependent phenomenon. In particular, a simple model for the calculation of the force for damage initiation, F_i, was proposed by Sjöblom [18]. The basic hypothesis was that first failure takes place when the shear stress τ along the thickness direction attains a critical value, τ_c, characteristic of the material under concern. In order to approximately evaluate τ, Sjöblom assumed a uniform distribution of this stress over a cylindrical surface of height coinciding with the specimen thickness, and radius r equal to that of the material-tup contact zone. The latter was calculated from the hertzian contact law, obtaining:

$$F_i = \frac{(2\pi \cdot t \cdot \tau_c)^{1.5} \cdot D_t^{0.75}}{k_c^{0.5}} \tag{1}$$

where k_c is the local rigidity of the material.
Eq. (1) was developed in [19], where the following relationship was drawn:

$$F_i = \delta \cdot D_t^{0.5} \cdot t^{1.5} \tag{2}$$

with the constant δ depending on the elastic constants of the composite, τ_c, and k_c.
Comparing eqs. (1) and (2), a seeming discrepancy is found in the effect of the tup diameter, whose exponent holds 0.75 in eq. (1), and 0.5 in eq. (2). This is due to the fact that in eq. (2) the link between k_c and D_t was explicitly expressed.
According to eq. (2), all the data deriving from tests carried out adopting different indenter diameters should converge to a single curve, when the term $F_i/D_t^{0.5}$ is plotted against t.

This is shown in Fig. 2 for the experimental results collected in the present research. Open and black symbols concern quasi-static and low-velocity impact tests, respectively.
As predicted by eq. (2), a single master curve is followed by the points associated with different D_t values. Further, the effect of speed is very limited, despite the viscoelastic nature of the matrix, from which τ_c is expected to mainly depend. Only in one case (see arrow in Fig. 2), representing a panel of small thickness (t=0.95 mm) loaded with a large diameter (D_t=19.8 mm) indenter, the superposition fails to be verified. This is somehow anticipated, because the flexural rigidity is low (low thickness), whereas the first failure load is relatively high (large tup diameter). Consequently, the curvature at first failure is large, and this substantially impairs the hertzian contact model, on which eq. (2) relies.

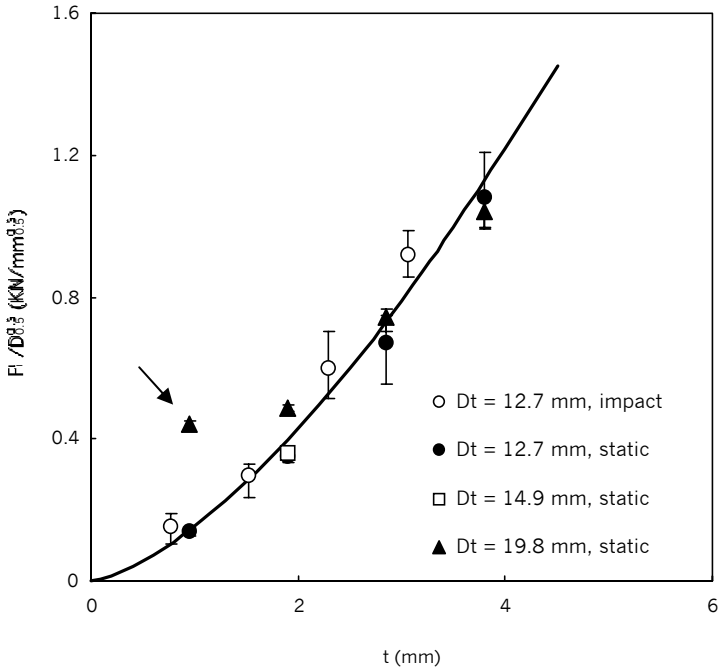

Fig. 2 - Effect of the laminate thickness, t, and tup diameter, D_t, on the first failure force, F_i.

The continuous curve in Fig. 2 is the graphical representation of eq. (2), whose constant was calculated by best fitting all the experimental data except the arrowed one, obtaining δ=0.152 KN/mm^2.
The previous results are in good agreement with those published in [20], where a large experimental data-base (about 350 specimens of different thicknesses and laminations, made of three types of basic laminae) was examined. In [14], the constraint conditions and impactor diameter were fixed. Nevertheless, the authors showed that F_i is dependent on $t^{1.5}$, and that the critical shear stress is a constant for laminates made of laminae having different orientations, although τ_c is strongly affected by the matrix type.

- Delamination extent and indentation
Fig. 3 shows the delamination extent against the imparted energy U for specimens of different thicknesses loaded with three different tup diameters. The delamination extent was measured from the projected area of delamination as revealed by ultrasonic C-scan.
Despite the large scatter affecting the experimental data, the trends observed seem to indicate that the influence of D_t on delamination development is quite limited: for given thickness and energy, the delaminated area is approximately the same, whichever the

indenter diameter. On the contrary, the laminate thickness is very important in determining delamination, with a larger delaminated area pertaining to the thicker laminate, even for a fixed energy level. This behaviour qualitatively supports the Liu model [11], according to which the tendency to delamination between two adiacent laminae is governed by the mismatch coefficient M, defined as:

$$M = \frac{[D_{11}(\theta_b) - D_{11}(\theta_t)]}{[D_{11}(0°) - D_{11}(90°)]} \tag{3}$$

where D_{11} is the first term of the [D] matrix, and θ_b, θ_t the orientations of the two adiacent laminae. Since D_{11} is a cubic function of the lamina thickness, eq. (3) predicts that, when (as in this work) two laminates having equal stacking sequence, but different lamina thickness are considered, the larger tendency to delaminate will be exhibited by the thicker one.

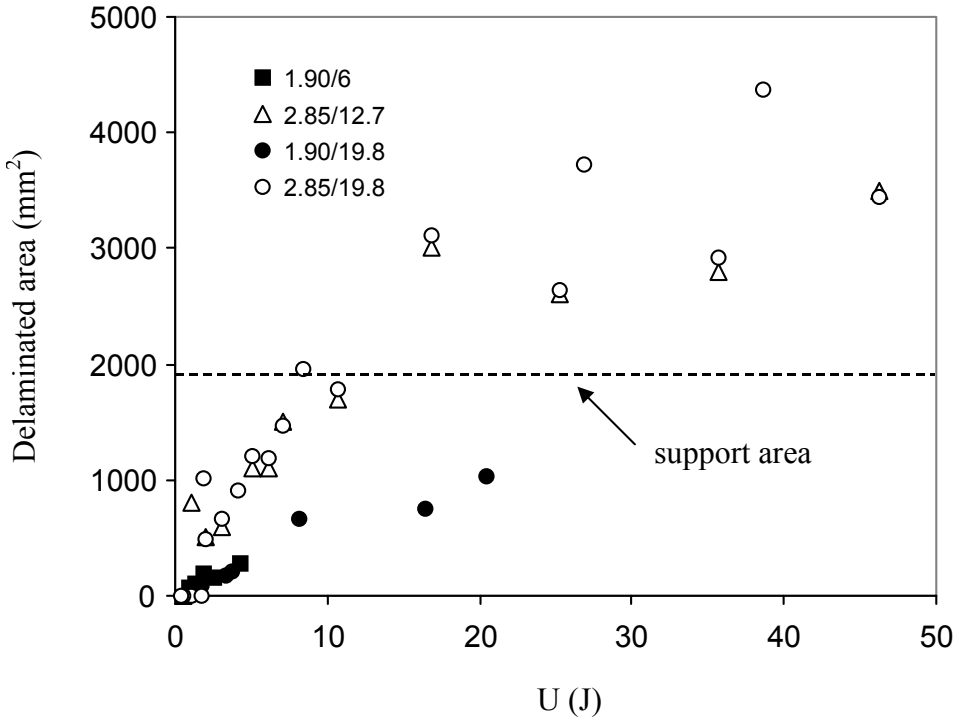

Fig. 3 - Delaminated area against energy, U. The symbols "a"/"b" in the legend indicate the panel thickness t ("a") and the tup diameter D_t ("b"), respectively, in mm.

As prevously stated, there is not a general agreement on the quantity determining delamination, with some researchers attributing it to the energy, and others to the maximum force F_{max} experienced during contact. Directly linking the mismatch coefficient to the force would be quite difficult, because the correlation between the mechanical behaviour of the material, constraint conditions, and tup geometry should be known. A more direct solution can be obtained assuming that two laminates identical, except for the lamina thickness, undergo a delamination proportional to M when the same energy is imparted to them. In this case, the ratio of the mismatch coefficient for the two laminates in Fig. 3 is given by $(2.85/1.90)^3$ =3.375. Consequently, for a given energy level, the thicker laminate should show a delaminated area 3.375 times larger than the thinner one.
To verify the previous hypothesis, all the delamination data in Fig. 3 concerning t=3.80 mm were divided by 3.375, obtaining an "equivalent delamination" allowing for a straightforward comparison of the two laminates (Fig. 4). As predicted by eq. (3), the

difference in behaviour attributable to the thickness, evident in Fig. 3, substantially disappears. Moreover, the linear relationship between energy and delamination extent, shown by other results available in the literature [13,14], appears for sufficiently low energy levels. Clearly, the linear correlation is violated when U is high. The reason is easily seen from Fig. 3: for U beyond 10 J, the delaminated area of the thicker specimens becomes larger than the support area, so that the effect of the constraint plays a significant role on delamination propagation. From the points in Fig. 3, delamination can propagate well beyond the support area (Fig. 5).

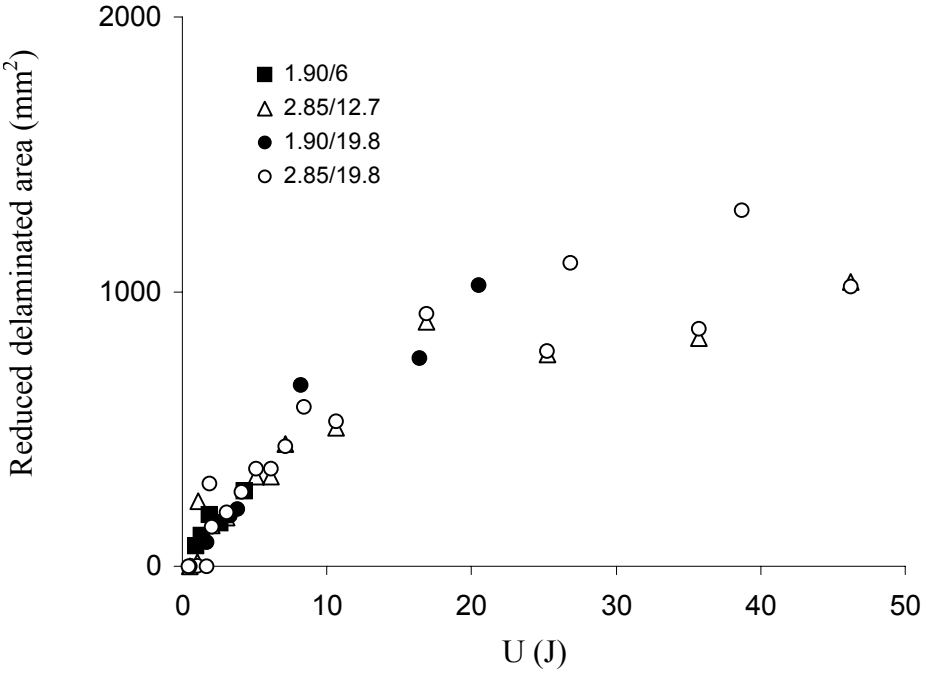

Fig. 4 - Reduced delaminated area against energy, U. The symbols "a"/"b" in the legend indicate the panel thickness t ("a") and the tup diameter Dt ("b"), respectively, in mm.

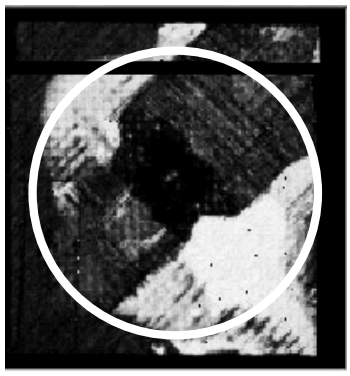

Fig. 5 - C-scan of a 2.85 mm thick laminate after an impact with an energy level U=27 J. White circle: support periphery.

The same delamination data in Figs. 3 and 4 are rearranged in Fig. 6, where the maximum force measured during contact has been used as the abscissa. All the points, irrespective of the panel thickness, sensibly converge to a single curve. Quite surprisingly, this occurs even for the data indicating a delamination extent overcoming the support periphery. According to Fig. 6, the larger delamination extent of the thicker laminate for a fixed U value simply depends on the larger contact force, deriving from its higher flexural rigidity and strength.

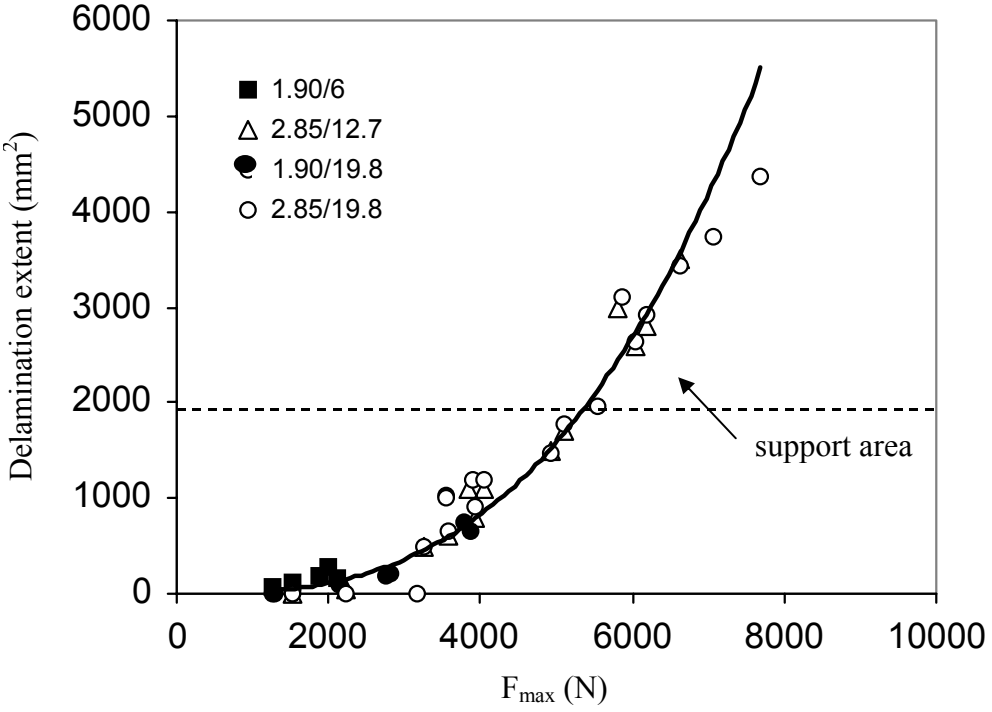

Fig. 6 - Delamination extent against maximum contact force, F_{max}.

The continuous line in Fig. 6 is the graphical representation of the empirical equation:

$$A = \eta \cdot F_{max}^{\beta} \tag{4}$$

where A is the delaminated area, and η, β two constants calculated by best fit, holding $\eta=3.13 \times 10^{-8}$ mm^2/N$^{\beta}$ and $\beta=2.89$. The results obtained suggest that these constants are independent of the tup diameter and panel thickness. On the contrary, η, β are presumably affected by the laminate type, since the delamination extent is influenced by the matrix nature [21] and lamination sequence [2]. Further, the validity of eq. (4) should be limited, for given t and D_t, by the condition $F_{max}>F_i$, where F_i is calculated by eq. (2). Applying this relationship to t=2.85 mm, D_t=19.8 mm (open symbols in Fig. 6), the value F_i = 3254 N is obtained, explaining the presence of the three points with zero delamination shown in the figure. Of course, these points were not accounted for in the evaluation of the constants η, β in eq. (4).

Obviously, if eq. (4) is assumed to be valid only when $F_{max}>F_i$, a discontinuity will be present in the law governing delamination growth. A possible physical explanation of this feature is yielded by the results published in [1,15], where it was noted that the first delamination propagation is probably unstable.

The solid curve in Fig. 6 is plotted for comparison purposes in Fig. 7. The points in the same figure represent the results of tests identical to those presented in Fig. 6, except for the support diameter, set equal to 100 mm. Clearly, the correlation between the data in Figs. 6 and 7 is poor: the delaminated area is considerably lower for the larger support diameter. Therefore, it can be concluded that the constants appearing in eq. (4) are dependent on this parameter.

The data in Fig. 7 also highlight another limit implicit in a force-based approach to delamination: when F_{max} attains about 6200 N, a large variability in delamination extent is observed. Rather than to the experimental scatter, this is attributable to the fact that

delamination continues to extend also beyond the maximum contact force, provided enough energy is available to further increase the displacement(Fig. 1).

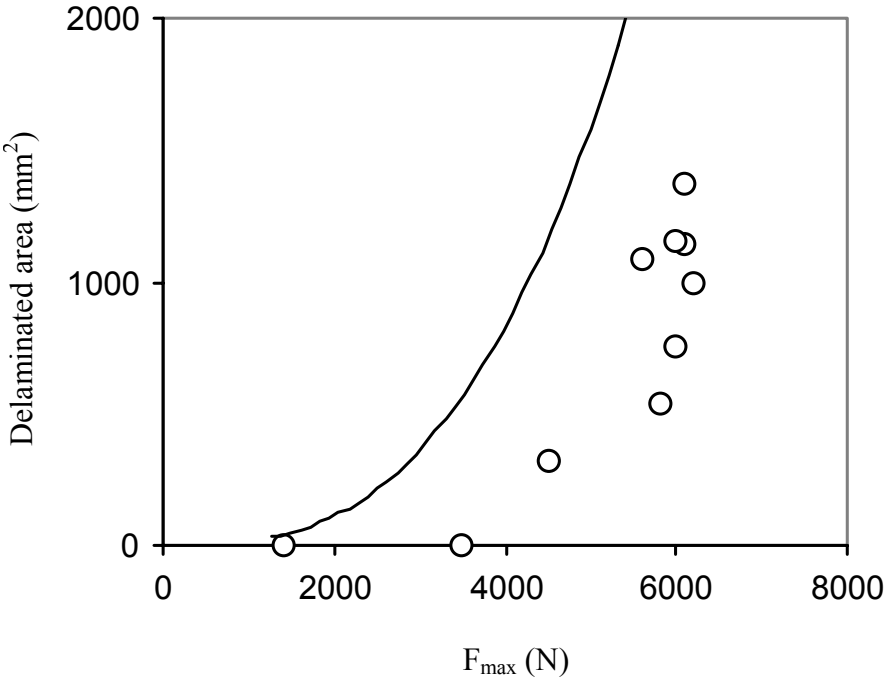

Fig. 7 - Delaminated area against the maximum force, F_{max}. Panel thickness t=2.85 mm; support diameter D=100 mm.

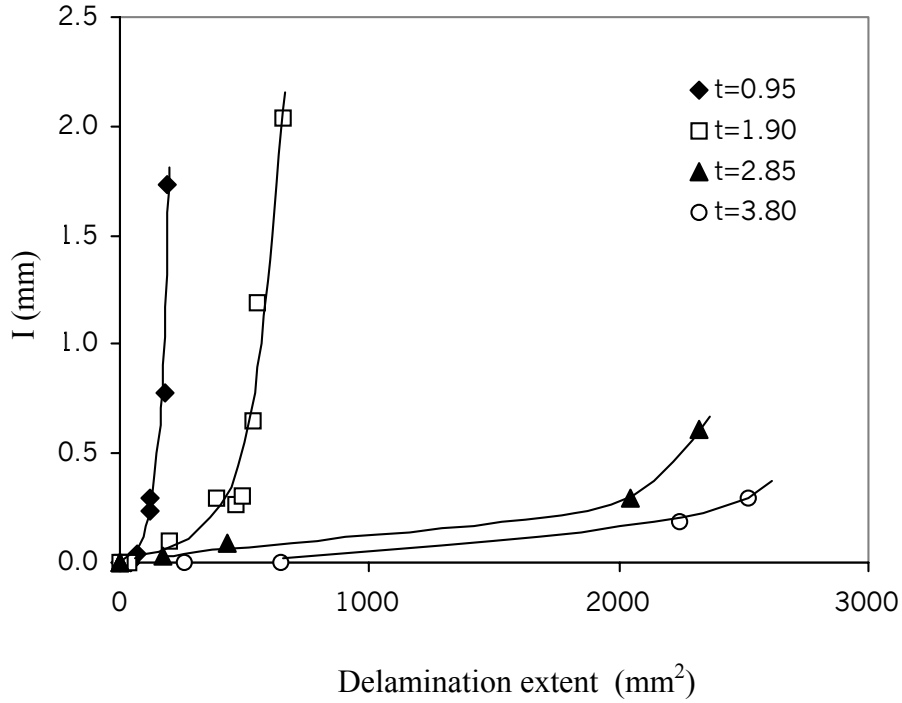

Fig. 8 - Indentation depth, I, against delaminated area for laminates of different thickness.

The previous considerations underline the complexity of the problem of delamination growth, for which adequate solutions are far from being available presently. Due to this, the laboratory results can be hardly transferred to practical cases, so that more costly tests on sub-structures are often required.

In Fig. 8, the relationship between the delaminated area and the measured indentation I for the different panel thicknesses is shown. The continuous lines were drawn by hand, to better evidence the experimental trends. The effect of the thickness on the A-I correlation is striking: thin laminates exhibit relatively limited delamination accompanied by large indentation; by contrast, thick laminates may suffer extensive delamination when the indentation is far from being clearly visible. For instance, when A is about 2500 mm^2 in the 3.80 mm thick panel, I holds 0.3 mm, lower than the limit indentation depth usually associated with BVID. Therefore, revealing an impact damage by visual inspection in a thick structure is much more complicated than in a thin laminate.

- Failure modes

There is general agreement among the researchers on the mechanisms of damage nucleation and development in a laminate subjected to a concentrated transverse load [10]. Beyond the first failure point, shear cracks, approximately oriented 45° with respect to the thickness direction, appear in the internal layers, and/or normal cracks driven by the bending stresses are generated in the laminae farthests from the impact point. These cracks are stopped at the interfaces between laminae having different orientations, where they give rise to delamination. The latter assumes a typical pine-tree shape along the material thickness, with the largest delaminated surface pertaining to the interlayer nearest to the back face of the panel. Sometimes, a reversed hat-shaped delamination has also been observed. For thick panels, the intense contact force may also result in small cracks immediately below the contact surface. With increasing energy, the failure phenomena involve also the fibres, starting form the surface opposite to the impact point.

Many of the previous features were revealed by the microscopic analysis carried out on the specimens loaded up to predetermined energy levels. However, also some specific characteristics, briefly discussed in the following, were noted.

Fig. 9a shows a schematic picture of the failure modes found in a thin panel quasi-statically loaded up to the first clearly perceivable load drop. A considerable damage, mainly consisting of shear cracks and delamination, is present in the specimen, whereas no local cracks are evidenced in the top layer just beneath the point of load application. Further, no normal cracks are detected at all.

In order to better estimate the conditions for damage initiations, some panels were loaded up to loads slightly lower than the first load drop. Even under these conditions, some damage was revealed by microscopy. An example is shown in Fig. 9b, from which it is seen that intralaminar cracks parallel to the interlaminar surfaces (arrow) were also occasionally found.

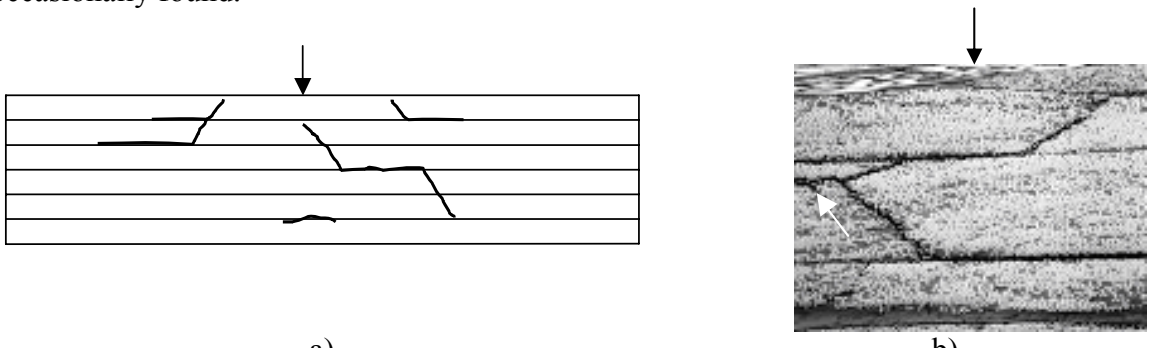

a) b)

Fig. 9 - First failure modes detected in the thinnest laminates (t=0.95 mm).

Local damage in the top layer due to the localised load was never found before evident first failure (as signalled by the F-d curve) in the 0.95 mm and 1.90 mm thick laminates. Instead, this occurred for the panels having t=2.85 mm and 3.80 mm. Apparently, these failures consisted of small cracks originating within the resin-rich areas of the fabric, and

did not interact with the subsequent delamination development. However, some fibre failures were sometimes found in their correspondence.
The presence of the fabric architecture in the bottom layer was effective in preventing the normal crack formation within them. In fact, this occurrence was noted after intense shear crack textures were found in the adjacent tape layers. Of course, increasing the energy level brought to an increase in the damage extent, and the first fibre failure within the bottom layer was detected well before the maximum load could be reached. Fracture surfaces of the panels loaded up to maximum force were characterised by a large delamination located at the interface between the bottom layer and the adjacent 45° layer, and complete collapse of the fibre bundles in the fabric (Fig. 10).

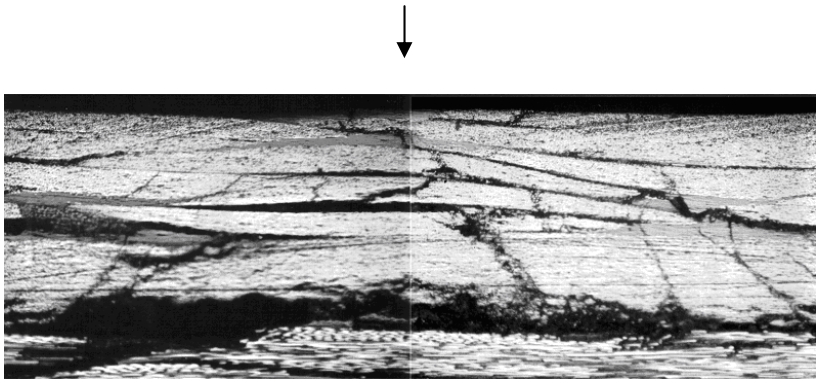

Fig. 10 - Damage in a 2.85 mm thick panel immediately beyond maximum load.

CONCLUSIONS

From the results presented and discussed in this work, concerning carbon fibre-reinforced panels of identical stacking sequences and different thicknesses loaded at the centre by a transverse load, the main conclusions are as follows.

- Increasing the panel thickness results not only in more intense contact forces, but also in larger displacements; of course, both these factors contribute to a higher energy carrying ability of the structure.
- Increasing the tup diameter is qualitatively similar to increasing thickness, with larger contact forces and displacements involved.
- The first failure load as perceived by a load drop in the force-displacement curve does not correspond to the actual force resulting in first damage occurrence within the material volume; this especially holds for thin laminates, for which detecting first failure from the macroscopic response is particularly difficult.
- A simple analytical tool, based on the hypothesis of a critical shear stress determining first failure, is helpful in predicting the first failure load.
- Both an energy-based criterion and a force-based criterion seem to work well in predicting the delamination extent.
- The visual inspection of thick laminates is quite difficult, because very small indentations may correspond to large delaminated areas in the material structure.

REFERENCES

[1] J.C. Pritchard and P.J. Hogg, "The role of impact damage in post-impact compression testing", *Composites*, Vol. 21, 1990, pp. 503-511.
[2] E.F. Dost, L.B. Ilcewicz and W.B. Avery, "Effects of stacking sequence on impact damage resistance and residual strength for quasi-isotropic laminates", ASTM STP 1110, T.K. O'Brien Ed., 1991, pp. 476-500.
[3] M.O.W. Richardson and M.J. Wisheart, "Review of low-velocity impact properties of composite materials", *Composites Part A*, Vol. 27A, 1996, pp. 1123-31.

[4] G.A. Bibo, P.J. Hogg, R. Backhouse and A. Mills, "Carbon-fibre non-crimp fabric laminates for cost-effective damage-tolerant structures", *Compos. Sci. Technol*., Vol. 58, 1998, pp. 129-43.
[5] S.L. Gao and J.K. Kim, "Effect of cooling rate on impact performance of carbon fibre/PEEK laminates", Proc. 8th Europ. Conf. Compos. Mater. (ECCM-8), Woodhead Publ., Cambridge, 1998.
[6] A.D. Curson, D.R. Moore and D.C. Leach, "Impact failure mechanisms in carbon fiber/PEEK composites", *J. Thermopl. Compos*., Vol. 3, 1990, pp. 24-31.
[7] M.S. Sohn, X.Z. Hu, J.K. Kim, L. Walker, "Impact damage characterisation of carbon fibre/epoxy composites with multi-layer reinforcement", *Composites Part B*, Vol. 31, 2000, pp. 681-91.
[8] N.K. Naik, R. Ramashimha, H. Arya, S.V. Prahbu, N. ShamaRao, "Impact response and damage tolerance characteristics of glass-carbon/epoxy hybrid composite plates", *Composites Part B*, Vol. 32, 2001, pp. 565-74.
[9] K. Dransfield, C. Baillie and Y.-W. Mai, "Improving the delamination resistance of CFRP by stitching - A review", *Compos. Sci. Technol*., Vol. 50, 1994, pp. 305-17.
[10] S. Abrate, Impact on composite structures, Cambridge University Press, Cambridge, 1998.
[11] D. Liu, "Impact-induced delamination - A view of bending stiffness mismatching", *J. Compos. Mater*., Vol. 22, 1988, pp. 674-92.
[12] G.A.O. Davies, X. Zhang, G. Zhou and S. Watson, "Numerical modeling of impact damage", *Composites*, Vol. 25, 5, 1994, pp. 342-50.
[13] W.J. Cantwell and J. Morton, "The influence of varying projectile mass on the impact response of CFRP", *Compos. Struct*., Vol. 13, 1989, pp. 101-114.
[14] Y.P. Siow and V.P.W Shim, "An experimental study of low velocity impact damage in woven fiber composites", *J. Compos. Mater*., Vol. 32, 1998, pp. 1178-202.
[15] W.C. Jackson and C.C. Poe, "The use of impact force as a scale parameter for the impact response of composite laminates", *J. Compos. Technol. Res*., Vol. 15, 1993, pp. 282-9.
[16] R. Teti, P. Buonadonna, V. Lopresto, G. Caprino, "Volumetric Ultrasonic NDE of damaged CFRP laminates", Acts of ECCM 10, Brugge, June 3-7 2002, Paper n. 346.
[17] D. Delfosse and A. Poursartip, “Experimental parameter study of static and dynamic out-of-plane loading of CFRP laminates”, Proc. 10th Int. Conf. On Compos. Mater. (ICCM10), Whistler, Canada, August 1985, pp. V-583-590.
[18]P. Sjöblom, "Simple design approach against low velocity impact damage", Proc. 32th SAMPE Symp., Anaheim, 1987, pp. 529-39.
[19] G. Caprino, A. Langella and V. Lopresto, “Prediction of the first failure energy of circular carbon fibre reinforced plastic plates loaded at the centre”, *Composites Part A*, Vol. 34, 2003, pp. 349-57.
[20] G.A. Schoeppner and S. Abrate, "Delamination threshold loads for low velocity impact on composite laminates", *Composites Part A*, Vol. 31, 2000, pp. 903-15.
[21] D. Delfosse and A. Poursartip, "Energy-based approach to impact damage in CFRP laminates", *Composites Part A*, Vol. 28A, 1997, pp. 647-55.